Thin Solid Films 518 (2010) 3101–3104

Contents lists available at ScienceDirect

Thin Solid Films

journal homepage: www.elsevier.com/locate/tsf

Transparent conducting Nb-doped anatase TiO_2 (TNO) thin films sputtered from various oxide targets

Naoomi Yamada [a,*], Taro Hitosugi [b], Junpei Kasai [a], Ngoc Lam Huong Hoang [a,c], Shoichiro Nakao [a,c], Yasushi Hirose [a,c], Toshihiro Shimada [a,c], Tetsuya Hasegawa [a,c]

[a] Kanagawa Academy of Science and Technology (KAST), Kawasaki 213-0012, Japan
[b] WPI Advanced Institute for Materials Research, Tohoku University, Sendai 980-8577, Japan
[c] Department of Chemistry, University of Tokyo, Tokyo 113-003, Japan

ARTICLE INFO

Available online 19 August 2009

Keywords:
Nb-doped TiO_2
Anatase
Sputtering
Ti_2O_3
Transparent conducting oxides

ABSTRACT

Transparent conducting Nb-doped anatase TiO_2 (TNO) epitaxial films were sputtered from TiO_2-, Ti_2O_3-, and Ti-based targets at various oxygen partial pressures (Po_2). Using the TiO_2- and Ti_2O_3-based targets, highly conductive films showing a resistivity (ρ) of ~$3\times10^{-4}\,\Omega$ cm could be formed without postdeposition treatment. In the case of the TNO films formed from the Ti-based target, reductive annealing had to be carried out at a temperature of 600 °C to achieve similar resistivity values. Thus, the use of oxide targets is preferable to obtain as-grown transparent conducting TNO films. In particular, the Ti_2O_3-based target is practically advantageous, because it offers a wide range of optimal Po_2 values at which ρ values of the order of $10^{-4}\,\Omega$ cm are achievable.
© 2009 Elsevier B.V. All rights reserved.

1. Introduction

The discovery of transparent conductivity in Nb-doped anatase TiO_2 ($Ti_{1-x}Nb_xO_2$; TNO) has increased the number of possible candidates for obtaining transparent conducting oxides (TCOs) [1]. Epitaxial films made from TNO exhibit a low resistivity (ρ) of $2–3\times10^{-4}\,\Omega$ cm with high optical transparency in the visible region [1,2], which is comparable to that of Sn-doped In_2O_3 (ITO) films that are the most extensively used TCOs. Even in polycrystalline form, TNO shows electrical and optical properties similar to those of epitaxial films [3–6], *i.e.*, ρ values of the order of $10^{-4}\,\Omega$ cm and optical absorption less than 5% in the visible region. In addition, TNO has unique characteristics that conventional TCOs, including ITO, ZnO, and SnO_2, do not have, such as a high activation ratio of Nb of more than 80% [1–6], a long plasma wavelength (*i.e.*, high transparency in the near-infrared region) due to a high optical permittivity of ~5.8 [7], a high refractive index of ~2.4 in the visible region [8], high anisotropic conductivity (*i.e.*, an anisotropic electron effective mass), which is attributed to the anisotropic nature of 3*d*-electron-based conduction band [9], and chemical stability under strongly reducing conditions such as hydrogen plasma atmosphere [10]. These unique characteristics could present the possibility of new applications wherein the conventional TCOs cannot be used.

Highly conductive TNO films have been grown by a magnetron sputtering (MSP) technique [4–6,11] as well as pulsed laser deposition (PLD) technique [1–3,12–15]. For the sputter growth of TiO_2-based films, a Ti-based metal disk or a TiO_2-based sintered disk is typically used as a target. Besides, a target based on the lower oxide Ti_2O_3 is also available [16]. The oxidation state of the target is believed to be important for the growth of transparent conducting TNO, because the conductivity of TNO is very sensitive to its oxygen stoichiometry; only oxygen-deficient TNO shows metallic conductivity [6,14,17,18]. The use of a lower-oxide-based target would expand the adjustable range of oxygen partial pressures during the growth of films and thus allow the growth of oxygen-deficient anatase phase more easily.

In this paper, we report on the growth of TNO epitaxial films by a sputtering technique using TiO_2-, Ti_2O_3-, and Ti-metal-based targets. The structural and electrical properties of the obtained films are discussed as functions of the oxygen partial pressure employed during deposition from each target.

2. Experimental procedure

$Ti_{1-x}Nb_xO_2$ ($x=0.06$) epitaxial films were grown by rf-MSP using $Ti_{1-x}Nb_xO_2$ (Nb:TiO_2), $Ti_{2-2x}Nb_{2x}O_3$ (Nb:Ti_2O_3), and $Ti_{1-x}Nb_x$ (Nb:Ti) targets (purchased from Toshima MFG Co., Ltd) and a single crystalline $LaAlO_3$ (LAO) substrate with (100) orientation. The target to substrate distance was 75 mm at the center of the target and substrate. The substrate temperature was set to 450 °C during the growth of the films. Sputtering was conducted in an Ar and O_2 mixture gas with various $O_2/(Ar+O_2)\equiv f(O_2)$ ratios (0–30%) at a total pressure P of 1.0 Pa. The oxygen partial pressure Po_2 during growth was defined as $Po_2=P\times f(O_2)$. The rf power applied to the target was maintained constant at 120 W during growth, and the deposition time was adjusted such that films with a thickness of ~150 nm could be obtained. The base pressure of our sputtering system (Canon ANELVA E200S)

* Corresponding author. Tel.: +81 44 819 2081; fax: +81 44 819 2083.
E-mail address: tg-yamada@newkast.or.jp (N. Yamada).

0040-6090/$ – see front matter © 2009 Elsevier B.V. All rights reserved.
doi:10.1016/j.tsf.2009.07.205

was ~5×10^{-5} Pa. Prior to each run of deposition, the target surface was sputter cleaned using pure Ar gas for 10 min and then presputtered for 5 min under film growth conditions.

Structural properties were analyzed using X-ray diffraction (XRD) with a two-dimensional detector (Bruker D8 Discover) Carrier transport properties including resistivity (ρ), carrier density (n_e), and Hall mobility (μ_H) were determined by carrying out four-probe and Hall measurements using a standard Hall bar geometry. The optical transmittance (T) and reflectance (R) were measured in a wavelength (λ) region from 0.3–2.5 μm using a UV–VIS–NIR spectrophotometer (JASCO V-670). All measurements were performed at room temperature.

3. Results and discussion

First, we describe the growth conditions employed for preparing single-phase anatase TNO epitaxial films from each target. Regardless of the target material, we could obtain epitaxial TNO films by adjusting Po_2, as shown in Fig. 1. In the case of the Nb:TiO_2 target, the anatase phase appeared at $Po_2\geq1.0\times10^{-3}$ Pa (Fig. 1(a)). When the Nb:Ti_2O_3 target was used, a higher Po_2, *i.e.*, $\geq1.0\times10^{-2}$ Pa, was required to grow the anatase phase (Fig. 1(b)). In the case of the Nb:Ti metal target, the Po_2 range required for the growth of the anatase phase shifted to the higher side, *i.e.*, $Po_2\geq1.0\times10^{-1}$ Pa (Fig. 1(c)). In the films prepared under the abovementioned conditions, impurity phases such as rutile TiO_2, Ti_nO_{2n-1}, and Nb_2O_5 were not detected, as observed in Fig. 1(a)–(c).

Next, we discuss the electrical properties of the sputtered TNO films. Fig. 2(a)–(c) show plots of ρ, n_e, and μ_H of the epitaxial TNO films grown from the oxide targets (Nb:TiO_2 or Nb:Ti_2O_3), as functions of Po_2. In Table 1, we show the transport properties of the most conductive films sputtered from each target. A minimum ρ value of $3.1\times10^{-4}\,\Omega$ cm ($n_e=1.4\times10^{21}\,\text{cm}^{-3}$, $\mu_H=14\,\text{cm}^2\text{V}^{-1}\text{s}^{-1}$) was achieved for the films deposited from the Nb:TiO_2 target at $Po_2=3.5\times10^{-3}$ Pa. A similar ρ value, $3.5\times10^{-4}\,\Omega$ cm ($n_e=1.6\times10^{21}\,\text{cm}^{-3}$, $\mu_H=11\,\text{cm}^2\text{V}^{-1}\text{s}^{-1}$), was obtained in the case of the TNO film grown from the Nb:Ti_2O_3 target at $Po_2=1.3\times10^{-2}$ Pa. In both cases, the transport properties showed a similar behavior with respect to Po_2. That is, each of ρ, n_e, and μ_H plotted against Po_2 showed a plateau in a low Po_2 range wherein the ρ values were of the order of $10^{-4}\,\Omega$ cm, $n_e>10^{21}\,\text{cm}^{-3}$, and $\mu_H>10\,\text{cm}^2\text{V}^{-1}\text{s}^{-1}$. Here, it should be noted that the plateau became wider in the case of the films deposited from the Nb:Ti_2O_3 target. In other words, the use of the Nb:Ti_2O_3 target effectively expanded the optimal Po_2 range wherein oxygen-deficient anatase can be obtained. As mentioned earlier, oxygen-deficient anatase is essential for preparing highly conductive TNO films [6,14,17,18].

As shown in Fig. 2, a further increase in Po_2 in excess of the optimal range resulted in a substantial increase in ρ, $>5\times10^{-3}\,\Omega$ cm. This was due to abrupt decreases in both n_e and μ_H to ~$4\times10^{20}\,\text{cm}^{-3}$ and ~$3\,\text{cm}^2\text{V}^{-1}\text{s}^{-1}$, respectively. Similar trends have been reported in the case of PLD-grown TNO epitaxial films [6]. Zhang et al. have attributed the decrease in n_e to the formation of acceptor-like defects such as oxygen interstitials (O_i) and/or titanium vacancies (V_{Ti}), which compensate for the carriers provided by Nb [6]. Further, it has been found by performing first-principles calculations that such acceptor-like defects have low formation energies under oxygen-rich growth conditions [19,20]. A recent resonant photoemission spectroscopy study has suggested that excess oxygen atoms, O_i, exist around Nb dopants and form acceptor-like impurity states in highly resistive, oxygen annealed TNO [17]. These results are consistent with the practical doping principles that *p*-type native defects are easily formed under host anion-rich growth conditions [21]. Hence, we speculate that the decrease in n_e at high Po_2 was

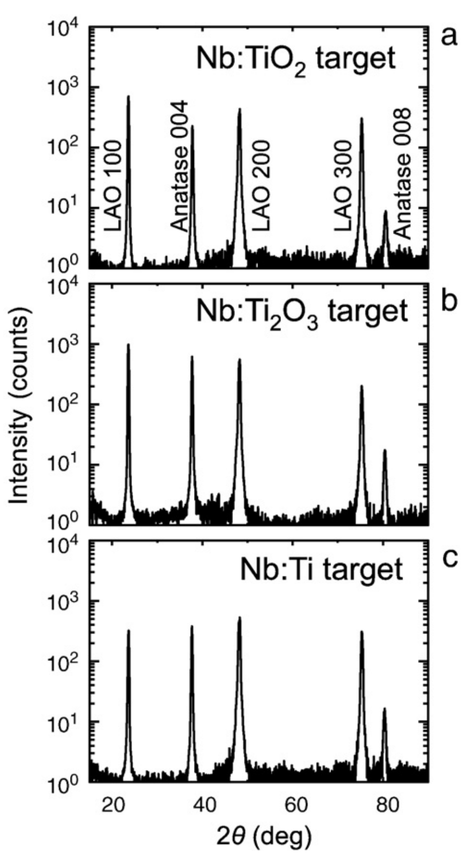

Fig. 1. XRD patterns of TNO epitaxial films sputtered from (a) Nb:TiO_2 target at $Po_2=1\times10^{-3}$ Pa, (b) Nb:Ti_2O_3 target at $Po_2=1\times10^{-2}$ Pa, and (c) Nb:Ti metal target at $Po_2=1\times10^{-1}$ Pa.

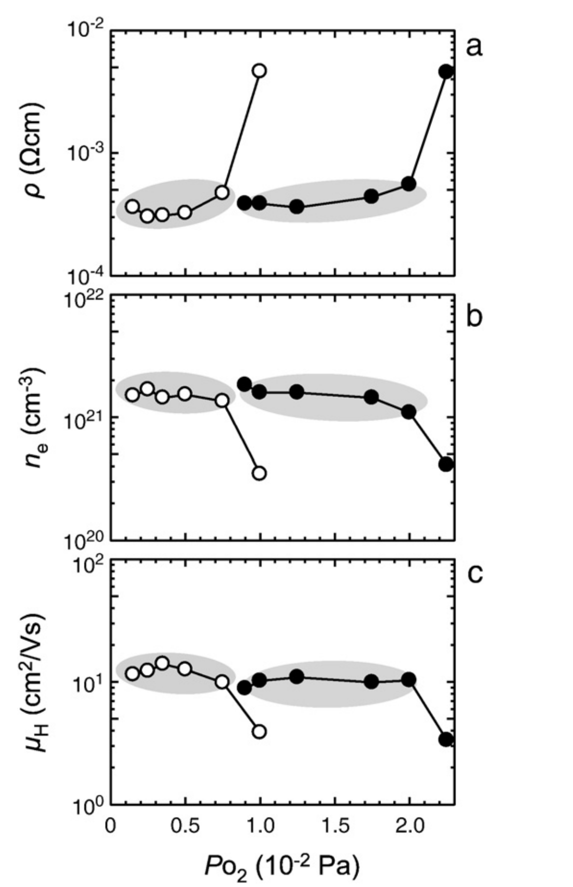

Fig. 2. (a) Resistivity ρ, (b) carrier density n_e, and (c) Hall mobility μ_H of TNO epitaxial films deposited from Nb:TiO_2 target (open circles) and Nb:Ti_2O_3 target (closed circles) plotted against Po_2. $\rho\leq1\times10^{-3}\,\Omega$ cm, $n_e\geq1\times10^{21}\,\text{cm}^{-3}$, and $\mu_H\geq10\,\text{cm}^2\text{V}^{-1}\text{s}^{-1}$ are attained at the shaded areas in (a), (b), and (c), respectively.

Table 1
Transport properties of TNO epitaxial films sputtered from Nb:TiO_2, Nb:Ti_2O_3, and Nb:Ti targets.

Target	Po_2 (Pa)	ρ (Ω cm)	ne (cm^{-3})	μH (cm^2/Vs)	Note
Nb:TiO_2	3.5×10^{-3}	3.1×10^{-4}	1.4×10^{21}	14	As-grown
Nb:Ti_2O_3	1.3×10^{-2}	3.5×10^{-4}	1.6×10^{21}	11	As-grown
Nb:Ti	1.0×10^{-1}	$>10^6$	–	–	As-grown
	1.0×10^{-1}	3.2×10^{-4}	1.6×10^{21}	12	Annealed[a]

[a] At 600 °C for 1 h in pure H_2 gas (1×10^5 Pa).

a consequence of the formation of such acceptor-like defects, especially O_i. These defects were expected to behave as electron scattering centers; therefore, low μ_H in the same Po_2 range could also be explained by the formation of such defects.

In contrast to the TNO films grown from the oxide targets, which can be made highly conductive by optimizing the growth conditions, the TNO films sputtered from the Nb:Ti metal alloy target were found to be always insulating with $\rho>10^6$ Ω cm. As shown in Table 1, an insulating film grown at $Po_2=1\times10^{-1}$ Pa was converted to a highly conductive ($\rho=3.1\times10^{-4}$ Ω cm) one by annealing under H_2 atmosphere at 600 °C for 1 h. This implies that the as-grown films contained a high concentration of O_i, which could be eliminated by H_2 annealing. It was difficult to grow conductive TNO films without O_i using metal targets, because the sputtering mode abruptly changed at low Po_2. Fig. 3 shows the deposition rate in the case of the Nb:Ti target, as a function of Po_2. The deposition rate suddenly increased in the vicinity of $Po_2\sim10^{-1}$ Pa, indicating that the sputtering mode changed to the metallic mode. In fact, the films obtained at $Po_2<1\times10^{-1}$ Pa had a metallic appearance.

The present results clearly show that oxide targets such as Nb:TiO_2 and Nb:Ti_2O_3 are preferable to obtain highly conductive as-grown films. In particular, the Nb:Ti_2O_3 target is useful, because TNO films having a low ρ value of the order of 10^{-4} Ω cm can be grown in a wide Po_2 range.

Finally, the optical properties of the optimized TNO film sputtered from the Nb:Ti_2O_3 target are briefly discussed. Fig. 4(a) compares T and R spectra of TNO/LAO with those of the LAO substrate. The figure shows that R increased and T decreased in the near infrared region, reflecting free-carrier absorption. Fig. 4(b) shows optical absorption (A) spectra estimated using the formula $A=1-(T+R)$. The A values of TNO/LAO around $\lambda=0.5$ µm were almost coincident with those of the bare LAO substrate, indicating that the TNO itself was highly transparent in the vicinity of $\lambda=0.5$ µm. Even in the other visible region, the difference in the A values between TNO/LAO and bare LAO was less than 0.13. Therefore, the use of Nb:Ti_2O_3 as a sputtering target did not degrade optical transparency.

4. Summary

In summary, TNO epitaxial films were grown by a sputtering technique using Nb:TiO_2, Nb:Ti_2O_3, and Nb:Ti targets. Highly conductive

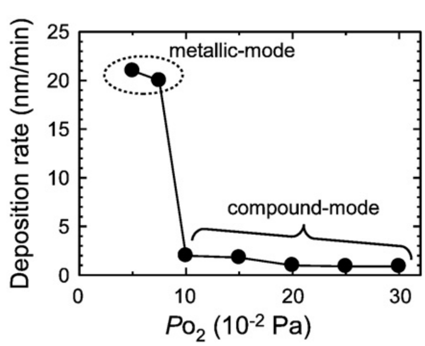

Fig. 3. Deposition rate as function of Po_2 (target, Nb:Ti).

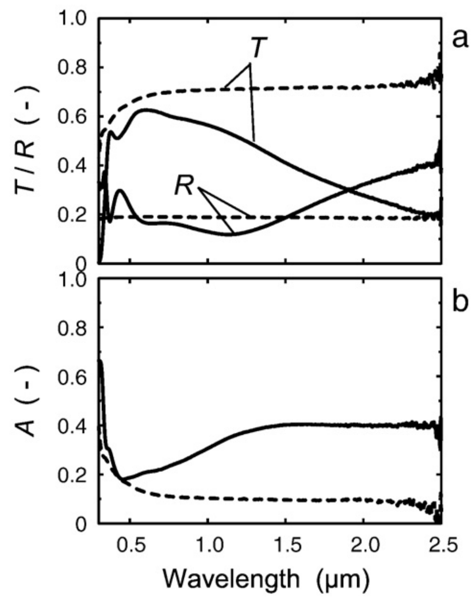

Fig. 4. (a) Transmittance T and reflectance R and (b) absorption A spectra of TNO film/LAO(100) sputtered from Nb:Ti_2O_3 target (continuous lines) and bare LAO substrate (broken lines). The film was grown at $Po_2=1.3\times10^{-2}$ Pa.

films showing $\rho\sim3\times10^{-4}$ Ω cm were grown from the oxide targets, Nb:TiO_2 and Nb:Ti_2O_3, without postdeposition treatment. On the other hand, the as-grown TNO films reactively sputtered from the Nb:Ti metal target showed an insulating behaviour and required H_2 annealing at high temperature (≥600 °C) for attaining $\rho\sim3\times10^{-4}$ Ω cm. Hence, the use of oxide targets such as Nb:TiO_2 and Nb:Ti_2O_3 is preferable to obtain as-grown TNO films with a low resistivity. Of the oxide targets used in this study, the Nb:Ti_2O_3 target is the better choice because it effectively expanded the optimal Po_2 range wherein low ρ values of the order of 10^{-4} Ω cm could be achieved.

Acknowledgements

This study was supported by MEXT Elements Science and Technology Project and a Grant-in-Aid for Young Scientist (B) 19760475, 2007.

References

[1] Y. Furubayashi, T. Hitosugi, Y. Yamamoto, K. Inaba, G. Kinoda, Y. Hirose, T. Shimada, T. Hasegawa, Appl. Phys. Lett. 86 (2005) 252101.
[2] T. Hitosugi, Y. Furubayashi, A. Ueda, K. Itabashi, K. Inaba, Y. Hirose, G. Kinoda, Y. Yamamoto, T. Shimada, T. Hasegawa, Jpn. J. Appl. Phys. 44 (2005) L1063.
[3] T. Hitosugi, A. Ueda, S. Nakao, N. Yamada, Y. Furubayashi, Y. Hirose, T. Shimada, T. Hasegawa, Appl. Phys. Lett. 90 (2007) 212106.
[4] N. Yamada, T. Hitosugi, N.L.H. Hoang, Y. Furubayashi, Y. Hirose, T. Shimada, T. Hasegawa, Jpn. J. Appl. Phys. 46 (2007) 5275.
[5] Y. Sato, H. Akizuki, T. Kamiyama, Y. Shigesato, Thin Solid Films 516 (2008) 5758.
[6] N.L. Hoang, N. Yamada, T. Hitosugi, J. Kasai, S. Nakao, T. Shimada, T. Hasegawa, Appl. Phys. Express 1 (2008) 115001.
[7] R.J. Gonzalez, R. Zallen, H. Berger, Phys. Rev. B 55 (1997) 7014.
[8] G.E. Jellison Jr., L.A. Boatner, J.D. Budai, B.-S. Jeong, D.P. Norton, J. Appl. Phys. 93 (2003) 9537.
[9] Y. Hirose, N. Yamada, S. Nakao, T. Hitosugi, T. Shimada, T. Hasegawa, Phys. Rev. B 79 (2009) 165108.
[10] M. Kambe, K. Sato, D. Kobayashi, Y. Kurokawa, S. Miyajima, M. Fukawa, N. Taneda, A. Yamada, M. Konagai, Jpn. J. Appl. Phys. 45 (2006) L291.
[11] M.A. Gillispie, M.F.A.M. van Hest, M.S. Dabney, J.D. Perkins, D.S. Ginley, J. Appl. Phys. 101 (2007) 033125.
[12] D. Kurita, S. Ohta, K. Sugiura, H. Ohta, K. Koumoto, J. Appl. Phys. 100 (2006) 096105.
[13] S.X. Zhang, D.C. Kundaliya, W. Yu, S. Dhar, S.Y. Young, L.G. Salamanca-Riba, S.B. Ogale, R.D. Vispute, T. Venkatesan, J. Appl. Phys. 102 (2007) 013701.
[14] S.X. Zhang, S. Dhar, W. Yu, H. Xu, S.B. Ogale, T. Venkatesan, Appl. Phys. Lett. 91 (2007) 112113.
[15] M.S. Dabney, M.F.A.M. van Hest, C.W. Teplin, S.P. Arenkiel, J.D. Perkins, D.S. Ginley, Thin Solid Films 516 (2008) 4133.
[16] M. Jerman, D. Mergel, Thin Solid Films 515 (2007) 6904.

[17] H. Nogawa, T. Hitosugi, H. Kamisaka, K. Yamashita, A. Chikamatsu, K. Yoshimatsu, H. Kumigashira, M. Oshima, S. Nakao, Y. Furubayashi, Y. Hirose, T. Shimada, T. Hasegawa, Proc. Mater. Res. Soc. Symp. Proc. 1074 (2008) 1074-I05-08.
[18] N. Yamada, T. Hitosugi, J. Kasai, N.L.H. Hoang, S. Nakao, Y. Hirose, T. Shimada, T. Hasegawa, J. Appl. Phys. 105 (2009) 123702.
[19] S. Na-Phattalung, M.F. Smith, K. Kim, M.-H. Du, S.-H. Wei, S.B. Zhang, S. Limpijumnong, Phys. Rev. B 73 (2006) 125205.
[20] H. Kamisaka, T. Hitosugi, T. Suenaga, T. Hasegawa, K. Yamashita, submitted to J. Chem. Phys.
[21] A. Zunger, Appl. Phys. Lett. 83 (2003) 57.